Laser and Particle Beams (2001), *19*, 55–58. Printed in the USA.

Measurement of XUV sources' wavefronts

S. LE PAPE,[1] PH. ZEITOUN,[1] P. DHEZ,[1] M. FRANÇOIS,[2] M. IDIR,[1] D. ROS,[1] AND A. CARILLON[1]

[1]Laboratoire de Spectroscopie Atomique et Ionique, Bât 350, Université Paris-sud, 91405 Orsay, France
[2]Institut d'Electronique et de Microélectronique du Nord, Université des Sciences et Technologie de Lille, avenue Poincaré BP 69, 59652 Villeneuve d'Ascq, France

(RECEIVED 30 November 2000; ACCEPTED 5 February 2001)

Abstract

New fields of X-ray source applications (X-ray laser and high order harmonic generation) could appear if an intensity higher than 10^{12} Wcm^{-2} is reached. Following this goal, we have started a complete investigation of the X-ray beam wavefront both numerically and experimentally. The first XUV wavefront sensor has been developed and tested on different XUV sources. For a better comprehension of the experimental results, a numerical work (ray-trace code) has been performed. We present and discuss the first results obtained on the X-ray laser at 21.2 nm.

1. INTRODUCTION

XUV sources, like high order harmonics generation or X-ray laser pumped either by a laser or by a capillary discharge are now used for applications (Da Silva *et al.*, 1995). Successful interferometer experiments have been realized to probe the electronic density of plasma or to visualize the surface default due to a high electrical field (Zeitoun *et al.*, 1998). But until now, nonlinear phoneme in the XUV range have not been observed because the required intensity of 10^{13} Wcm^{-2} to induce those phenomena has not been reached. To reach this intensity, experiments to focus an X-ray laser using a Bragg–Fresnel lens have been tried unsuccessfully (Zeitoun *et al.*, 1998). To reach a diffraction limited spot size, the incident wavefront has to be very regular; that is why we start to study the shape of the XUV source wavefront. For this purpose, we developed the first XUV wavefront sensor based on the Shack–Hartmann (SH) principle. We present in this article the SH principle and the first result obtained with an X-ray laser at 21.2 nm.

SHACK–HARTMANN PRINCIPLE

We have decided to use a Shack–Hartmann wavefront sensor to study the beam quality of the XUV sources. This wavefront sensor is currently used in visible light to analyze, for example, large mirror defaults on telescopes, or the heating of mirrors on high power laser installation. It was preferred to other techniques, such as an interferometer, for two main reasons. This wavefront sensor can still give information on the full beam quality when the source is only partially spatially coherent; that is, of course, not the case with an interferometer. The second reason is that the sensor is experimentally easy to use, which is an important argument for studying several sources.

The Shack–Hartmann principle is to sample the beam using a lens array. Each lens focuses the light on a detector that is placed at the focal point, providing local information on the shape of the wavefront. Indeed if the incident wavefront is parallel to the plane of the lens, then the focal spot will be on the optical axis of the lens. If the incident wavefront is tilted with respect to the lens plane, the focal spot will move away from the optical axis (Fig. 1). One measures those displacements of the focal spots by comparing them to a reference wave that is supposed to be a spherical wave, to map the tilt of the wave vectors. This reference wave is generated by the diffraction of a very small pinhole. This reference wave has not yet been made for the experiment on the X-ray laser at 21.2 nm. That is why we present only relative displacement of the focal spots.

In addition, if the source is fully coherent on the full beam dimension, one can reconstruct the wavefront surface, because it exits a phase relation between all the points of the wavefront sensor.

At this wavelength transmission, the lens should be made of a very thin membrane, which means that all the lenses could not be coplanar. To avoid this problem, we use Bragg–Fresnel lens (Fig. 2); the coplanerity of the lens is then only limited by the planerity of the substrate. In addition, those Bragg–Fresnel lenses do not have any geometrical aberrations which would disturb the measurement. An Mo/Si multi-

Address correspondence and reprint requests to: Sebastien Le Pape, Laboratoire de Spectroscopic Atomique et Ionique, Bât 350, Université Paris-sud, 91405 Orsay, France. E-mail: sebastien.le-pape@lsai.u-psud.fr.

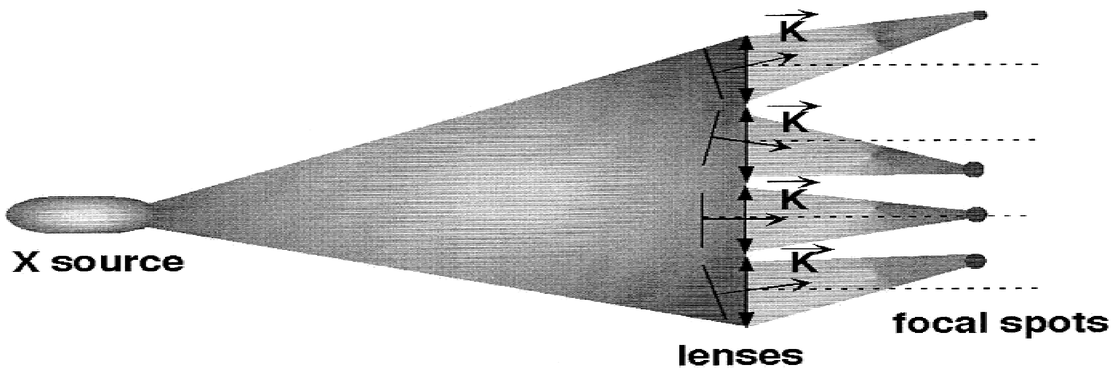

Fig. 1. Shack–Hartmann principle.

layer has been coated on the substrate surface. The array is composed of 12×10 lenses. Each lens has nine grooves, the focal lens is 75 cm, their diameter is 700 μm, and the last groove size is 13 μm, which leads to a focal spot around 100 μm.

We used this wavefront sensor for the first time to study an X-ray laser pumped by a laser. In the case of an X-ray laser pumped by a laser, the coherence length at 2.5 m from the source is typically around 200 μm, which means that this wavefront sensor will provide a map of the tilt of the wave vector.

3. RESULTS

This experiment was made at the LULI with a well-known double-pass X-ray laser at 21.2 nm. The plasma parameters are as follows: an IR (1.06 μm) laser irradiates a massive flat iron target. Two 600-ps Gaussian pulses are used with a time delay of 5.6 ns. The first and second pulse intensities are 2×10^{11} Wcm^{-2} and 10^{13} Wcm^{-2}, respectively. The laser is focused on a 20×0.1 mm^2 focal line.

In the case of the X-ray laser, the tilt of the wave vectors is due to the refraction in the amplifying medium because of the strong electronic density gradient. To attenuate this refraction in the plasma we use a prepulse before the main pulse. This prepulse creates the preplasma; therefore the main pulse interacts with plasma.

We have changed the prepulse level to study this dependence. During that experiment we first used a CCD after placed a phosphor (see Fig. 3). But the CCD chip was too small to catch the full beam, which is why we changed the detector using an image relay (see Fig. 4). We can see on this image the footprint of the beam due to the reflection of the multilayer deposed on the whole substrate. We can also see

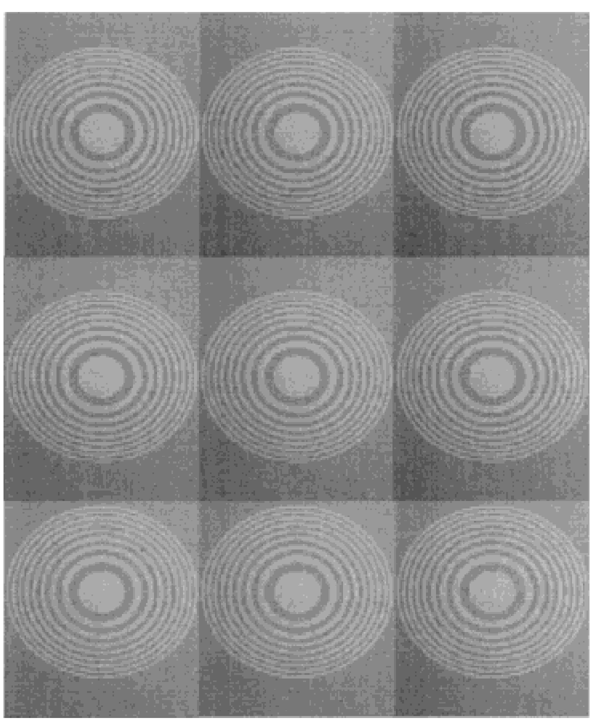

Fig. 2. Array of Bragg–Fresnel lenses.

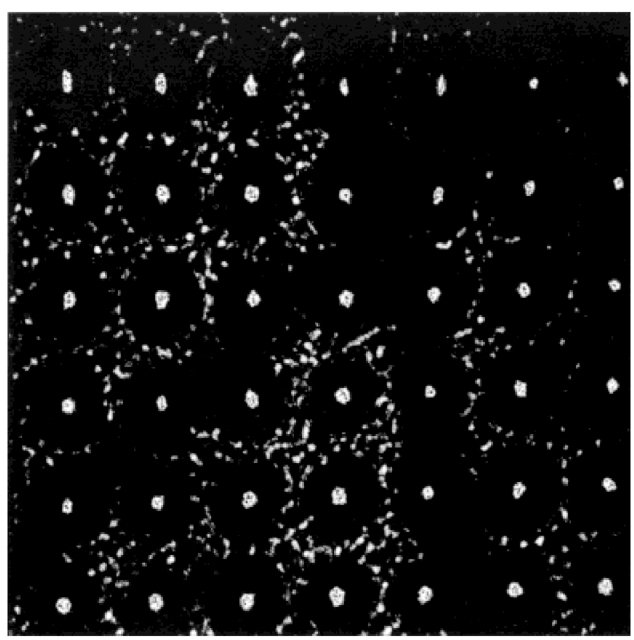

Fig. 3. Image obtained with a CCD camera.

https://doi.org/10.1017/S0263034601191081 Published online by Cambridge University Press

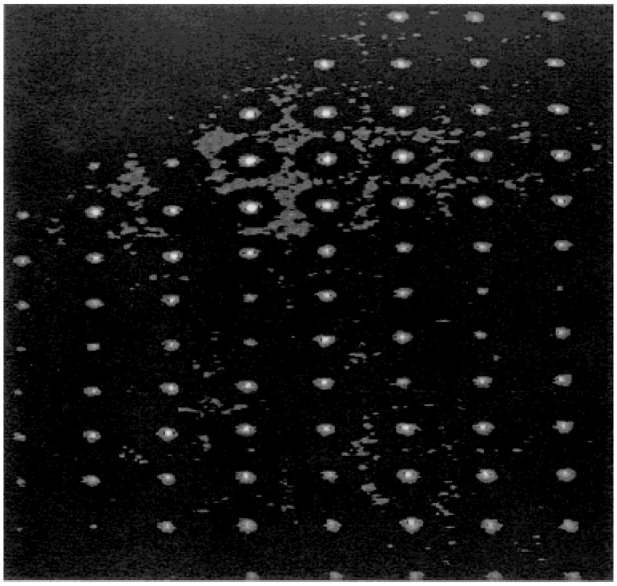

Fig. 4. Image obtained with an image relay.

the cross wires that are used to align the X-ray laser beam on the optic. This change of detector decreases the resolution of the wavefront sensor by a factor 10.

Despite this loss of resolution, we can observe the modifications of the wave vector tilt in subtracting the image obtained for two different levels of prepulse. Figure 5 is the subtraction of two images for the corresponding prepulse level $5 \times 10^{-3} \times$ Ip and $9 \times 10^{-3} \times$ Ip; Ip is the intensity of the main pulse. Note that the subtraction of two images for the same prepulse level results in a flat signal.

We remark in Figure 5 that the focal spot displacements are not uniform on the surface of the detector. This nonuniformity proves that those movements are not due to a misalignment of the X-ray laser, which would have led to a uniform movement, but to a local modification of the refraction. Figure 6, which is a zoom in of the previous image, clearly shows the local displacement of the focal spots in the coexistence of two nearby focal spots.

This modification of the prepulse level induced a lateral displacement of the focal spot that is due to smoother electronic gradient in the lateral plane. Despite the loss of resolution this wavefront sensor was sensible to a small change of the prepulse level, and those measurements exhibit the expected behavior.

4. CONCLUSION

The aim of this first experiment was to validate the principle of the Shack–Hartmann wavefront sensor in the XUV range. Even with the use of an inadequate detector, this wavefront sensor was sensible to a change in the prepulse level that is not visible on footprint. The wavefront sensor resolution for this experiment was $\lambda/100$ (λ of the XRL); this resolution could be improved, first by using an XUV CCD with a chip that is large enough to catch the full beam, and second by optimizing the design of the lens array.

For better comprehension of those experimental results, we have developed a 3-D ray-tracing code that gives directly comparable data with the SH data. This code is a 3-D

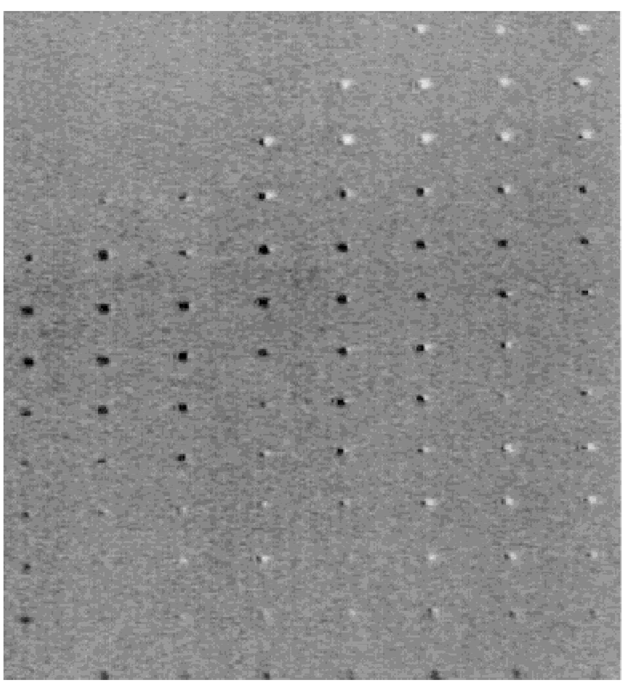

Fig. 5. Subtraction of two shots.

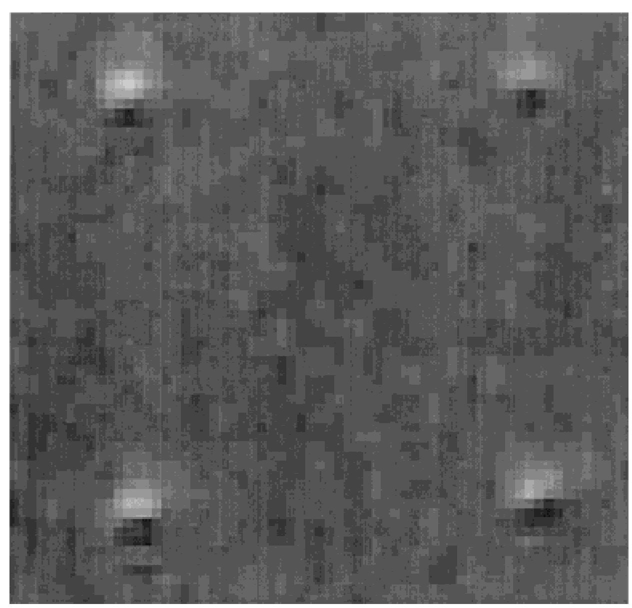

Fig. 6. Zoom in.

https://doi.org/10.1017/S0263034601191081 Published online by Cambridge University Press

description of the beam propagation, including the half cavity mirror. It is based on the integration of the ray equation and on the calculation of the intensity along the plasma. It works as a postprocessor of the hydrodynamic/atomic code "EHYBRID," which calculates the temporal evolution of the plasma. Results of the simulation are presented in a companion paper (Le Pape & Zeitoun, 2001, p. 137, this issue).

REFERENCES

Da Silva, L.B. *et al.* (1995). *Phys. Rev. Lett.* **74**, 3991–3994.

Le Pape, S. & Zeitoun, Ph. (2001). *Laser Part. Beams* **19**, 137.

Zeitoun, Ph. *et al.* (1998*a*). *Nucl. Inst. Meth. Phys. Res A* **416**, 189.

Zeitoun, Ph. *et al.* (1998*b*). *Proc. 5th Int. Conf. on X-ray Lasers.*

https://doi.org/10.1017/S0263034601191081 Published online by Cambridge University Press